Journal of Geoscience and Environment Protection, 2017, 5, 155-175
http://www.scirp.org/journal/gep
ISSN Online: 2327-4344
ISSN Print: 2327-4336

Synoptic-Thermodynamic Analysis of Pervasive Hailstorm Case Study: Tehran, March 30, 2015

Mahmoud Ahmadi*, Farzaneh Jafari, Tayebeh Akbari Azirani, Abbasali Dadashiroudbari

Shahid Beheshti University, Tehran, Iran
Email: *ma_ahmadi@sbu.ac.ir

How to cite this paper: Ahmadi, M., Jafari, F., Azirani, T.A. and Dadashiroudbari, A. (2017) Synoptic-Thermodynamic Analysis of Pervasive Hailstorm Case Study: Tehran, March 30, 2015. *Journal of Geoscience and Environment Protection*, **5**, 155-175.
https://doi.org/10.4236/gep.2017.59012

Received: July 23, 2017
Accepted: September 10, 2017
Published: September 13, 2017

Abstract

The objective here is to assess the atmospheric evaluations with respect to the perilous hailstorm phenomenon in Tehran. To accomplish this study, the available data regarding 9 (WW) present weather codes that reveal the hailstorm phenomenon with different intensities in 3 hrs observations for 6 meteorological stations of Tehran and vicinity for the period between 1985-2015 are applied. It is revealed that hail occurrence in Tehran is at its maximum in transition seasons of spring and fall between the hrs. 6 - 18 (UTC). It is found that the instability indexes intensify in the afternoon with a higher atmospheric flotation indicative of the possibility in occurrence of thunder hailstorm. Synoptic assessments point to the fact that the synoptic pattern created this thunder storm due to expansion of two: low-pressure cores over Arabia and North-Europe and the cold high-pressure over South Russia with a NS orientation have developed an intense pressure gradient over Tehran province. The study area being located at the left exit of sub-tropical jet stream has made a Baroclinic atmosphere condition on Tehran province. Access to great humidity resources of Mediterranean and Black seas and a drastic decrease of temperature at the upper level of the cloud verifies the hail occurrence on March 30th of 2015 in Tehran.

Keywords

Hail, Thermodynamic Indexes, Synoptic, Blocking Systems, Tehran Province

1. Introduction

Hailstorm is one of devastating climatic phenomena that damages including agriculture in specific, detrimental to transportation etc. The occurrence of this phenomenon depending on certain, topographic and atmospheric conditions [1] and the damage rates differ with respect to hail size, its fall intensity and

space-time condition and the spatial centers [2]. This is a form of precipitation in the form of ice corresponding to thunderstorm's category in an unstable atmosphere [3], by forcing added moisture at low-level and presence of strong vertical shear wind [4], in strong advecting conditions together with freezing the lower layer air masses in the atmosphere with fronts containing two different air masses at the upper level of the jet stream [5] and, often they form in cumulonimbus clouds that include minimum hail size of 5 mm [6] with a maximum hail size of 10 cm [7].

Intensity in global warming most probably could increase the frequency of climatic extremes, hail in specific which is a devastative occurrence directly effecting insurance and economic industries. An increase in greenhouse gas emission has been caused changing the climatic parameters in a significant manner at global scale. The Intergovernmental Panel on Climatic Change [8] [9], in its 5th assessment named (AR5) concludes that human intervention is the essential contributor to the changes in climate system. Monitoring these changes indicate the changes in frequency and intensify the normal trend of extremes in daily temperatures at global scale from middle 20th century [10]. In a broad perspective all regions of the globe (except small regions in the North Atlantic Ocean) have experienced the global temperature increase [8]. Then the probable effect of global warming could increase the frequency of occurrences such as hail [11] and intensify their damages [12].

Alarming on hail occurrence to the vulnerable areas must be issued in an effective manner as to mitigate the possible loses. The Doppler Weather Rader (DWR) can issue the alarm 15 min prior to occurrence, while to better identify this devastating atmospheric phenomenon its modeling should take priority in related studies in order to develop more appropriate parameter(s) in expanding water vapour/water liquid conversion to ice to prevent hail occurrence. The applied synoptic predictive parameters [13] are of essence but not sufficient on their own. The pre-awareness from the occurrence of this phenomenon provides a rich perception of its mechanism, thus, the necessity to run studies on simulating this phenomenon.

The available studies on this important topic consist of two major categories: 1) The changes in the temporal-spatial variation of hail and 2) finding causation through case studies to determine the hail occurrence patterns. The authors in the first category consist of: [14] who determined the frequency and intensity of hail occurrence by applying a 10-year data (1987-1996) data as to the hail hazard plan for France. Similar study is run by [1] in Canada; by [15] in Friuli Venezia Giulia fields; by Friuli Venezia Giulia, [16] in two Australian states of Sydney and South wales and by [17] who studied the spatial context of hail occurrence in both the 19th and 20th centuries in Moravia and Silesia regions of Czech Republic. The pattern change in thunderbolt and hail occurrence relevant to atmospheric features in SE Germany is assessed by [18] for the period within the years 1974-2003, where the results indicate an incremental pattern in thunder-

bolt and hail occurrence. In a study run by [19] based on the data form 25 meteorological stations for the period (1960-2010) it is revealed that in general hail occurrence in the transitional seasons of spring and fall with its occurrence core at the heights of NE and W Iran with the thunder occurrence in SE, S and central Eastern regions.

The second category consists of: in a digital and synoptic simulation of hailstorm recorded on April 14, 1999 in Sidney the authors [20] concluded that presence of a relatively high energy transfer potential has had a great contribution. The Synoptic and thermodynamic patterns of hail occurrence at North of Greece in hot season is assessed in [21] revealing that the flows and SW trough had the most influence on hail occurrence. The low shear pressure of climatic features in the north hemisphere with an emphasis on NE China that cause hailstorm, is found to be related to cyclic systems, fronts and low pressure shear [22]. The unusual hail occurrence of June 24, 2006 in Boulder, Colorado is assessed by [23] an [24] have assessed the same occurrence on 16th May, 2010 in Oklahoma.

As for Iran, since this phenomenon is specific to the period within spring and fall which seasonal change its occurrence in spring when all orchards are in blooming state and people take short trips to enjoy spring the potential of financial and human damages is high. Accordingly, comprehensive and accurate studies on state part could contribute to better management at national level in this respect.

2. Data and Methods

Megacity of Tehran is the biggest city, is the capital and is the center of Tehran province, of and in Iran. Its total area is 730 km^2, is the 25th highly populated and 27th biggest city of the world. The geographic coordinates are 35˚41'21.11"N and 51˚23'20.30"E at 2000 m for Maximum sea level at its north to 1200 m in center And 1050 in its south. To assess the hailstorm occurrence here, the available data codes 99.96, 94, 93, 90, 89, 88, 87, 27 (WW) of **Table 1**, in a clock wise manner

Table 1. The characteristics of hail's codes [26].

WW	Code
Shower(s) of hail, or of rain and hail	27
Shower(s) of snow pellets or small hail, with or without rain or rain and snow mixed (slight)	87
Shower(s) of snow pellets or small hail, with or without rain or rain and snow mixed (moderate or heavy)	88
Shower(s) of hail, with or without rain or rain and snow mixed, not associated with thunder (slight)	89
Shower(s) of hail, with or without rain or rain and snow mixed, not associated with thunder (moderate or heavy)	90
Slight snow, or rain and snow mixed or hail at time of observation	93
Moderate or heavy snow, or rain and snow mixed or hail at time of observation	94
Thunderstorm, slight or moderate, with hail at time of observation	96
Thunderstorm, heavy, with hail at time of observation	99

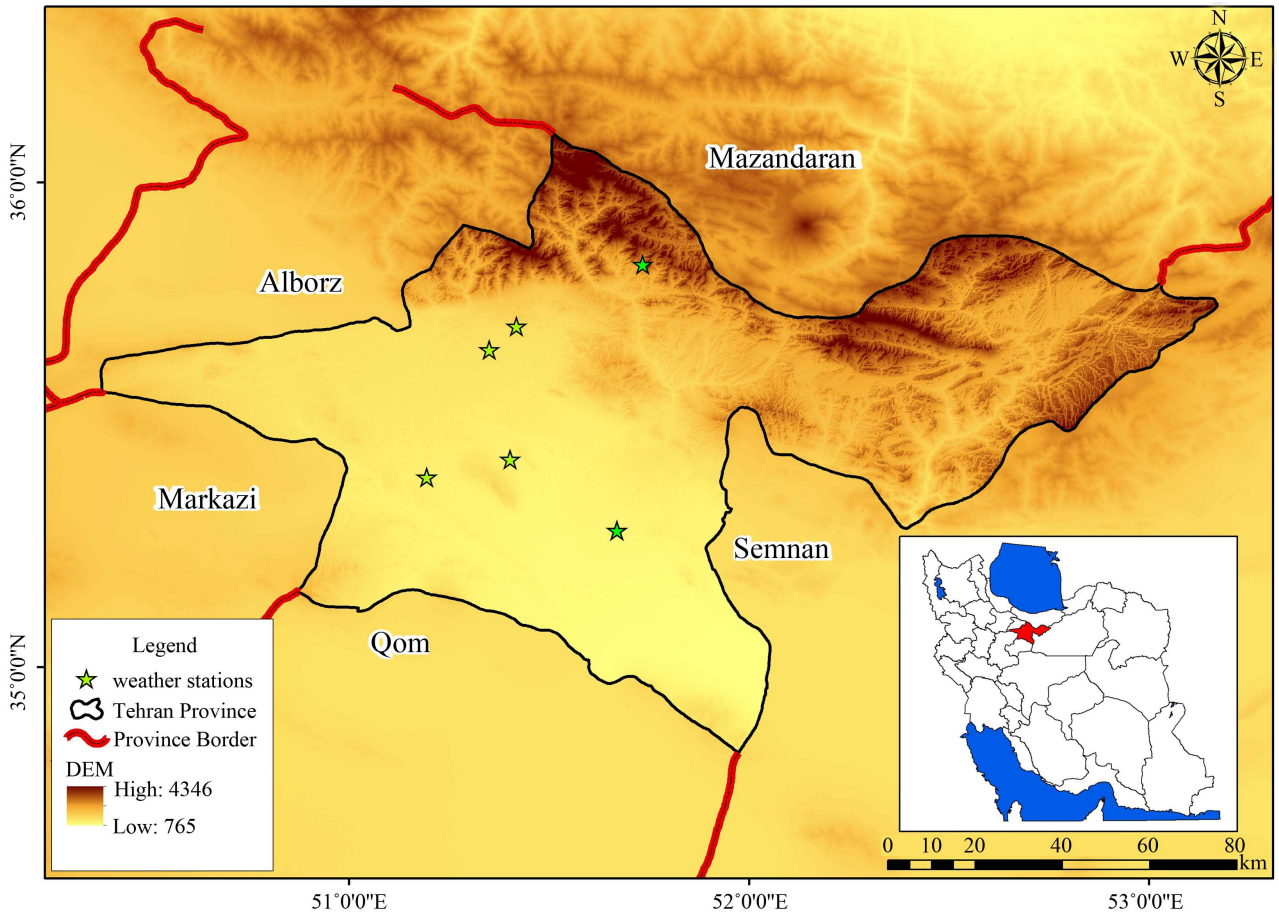

Figure 1. Geographical distriction of the stations in the studied area.

(standard observations of 3 h intervals) at meteorological stations of Mahabad, Rey, Varamin, Geo-physics, Pakdasht and Aghdasieh are applied for a 30 year period of 1985-2015), (**Figure 1**). Following this statistical assessment, the heaviest and the highest of hailstorm occurrences occurred in 30th March, 2015. According to the reports provided by the Agricultural institutions of Tehran province, this one time occurrence damage to the orchards of Shahriar, Malard, Rey and Shemiranat was estimated at $39 mil (2017 exchange price).

In the same report 53,000 Hectares of gardens with orchards were affected with an estimation of 25% in Shahriar and 15% in Malard, Rey and Shemiranat [25].

In assessing the precipitation extreme occurrence, the scale of atmospheric synoptic conditions contributes significantly. To determine the synoptic pattern for the selected day in the study area the researched data with 2.5 × 2.5 networking from national (NCEP/NCAR) in an observation of 6 hrs period is run for pre and post occurrence days. The applied data consist of sea surface pressure, geopotential height, orbital (U) and Meridian (V) and vertical velocity (Omega) for the available levels.

In the next step to assess the dynamic and thermodynamic conditions of hail

occurrence in the select day the higher atmospheric level of Radiosand data of Mehrabad meteorological station (40,754) for two observation times at 0 o'clock and 12 o'clock is obtained from University of Wyoming at the following inconsistency indexes. Then instablity indexces are calculated which are discussed in the following section. The Modis data is applied in order to run precise assessment of liquid and icy clouds'spath and to calculate cloud's temperature.

2.1. Showalter Index (SHOW)

This index is calculated through an ascending closed circuit air package at 850 hPa to 500 hPa [27]. This index is indicative of general stability for air masses and measures the possibility of instability in term of ˚C between 850 to 500 hPa levels according to Equation (1):

$$\text{SHOW} = T_{E500} - T_{p500} \tag{1}$$

where, SHOW (SI) is the index (in ˚C), T_{E500} is the environment heat at 500 hPa level (˚C) and T_{p500} is the air parcel temperature at 500 hPa (˚C), provided that the first air parcel began to ascend from 850 hPa level. The more negative the SI, the stronger the instability, thus, more floatation which ends in upwards trend of the parcel for PBL [28].

2.2. KINX Index

This index is a basic ratio for thunderstorm potential on temperature degree vertical lapsrate, volumes and vertical span of humidity at low atmospheric levels. To calculate K the three determined levels of 500, 700 and 850 hPa are applied through Equation (2):

$$KI = \left(T_{850} - T_{500}\right) + TD_{850}\left(T_{700} - TD_{700}\right) \tag{2}$$

where, T and T_d are the temperature and due point temperature per (˚C) in mentioned levels respectively [29].

Relation one on the right is temperature decrease pattern where, if the volume is big and positive, instability prevails. Relation to the same side is indicative of humidity at 850 hPa where, if it is high, if contributes more to instability. Relation 3 (with negative sign) has calculated dry air at 700 hPa and if the volume is high there exist dry air at that level, thus, a negative on instability [29].

2.3. Boyden Index

This index is designed by [30] considering temperature at 700 milibar to evaluate the thunderstorms at the front crossings. In this index. The evaluation differences at 700 and 1000 hPa levels indicates that thickness of this layer corresponds to its average temperature. This index is expressed as follows:

$$\text{BoydI} = 0.1\left(Z_{700} - Z_{1000}\right) - T700 - 200 \tag{3}$$

2.4. KO Index

This index introduced by [31] describes the instability potential between the

upper and lower levels of the atmosphere. This index is based on temperature potential, Equation (4):

$$Ko = 0.5\left(\theta_{e,500} + \theta_{e,700}\right) - 0.5\left(\theta_{e,850} + \theta_{e,1000}\right) \tag{4}$$

This index is at its lowest volume when cold and dry air covers hot and moist air.

2.5. Convective Available Potential Energy Index (CAPE)

This index reveals the maximum possible kinetic energy of instable air parcel, regardless of water vapor effect and condensate water in floatation. This index is one of the major indexes in predicting instability within one or two days and is not able to determine the factors involved instability. High volume of CAPE indicates the existence of more difference between the environment and the ascending air package temperatures. The more this difference is the stronger the floating power and ascending intensity [32]. Regions with negative surface are considered as Convective Inhibition Energy (CIE), thus, a surface the air parcel of which is colder in relation to its surrounding environment. Equation (5):

$$\mathrm{CAPE}\left(\mathrm{J}\cdot\mathrm{kg}^{-1}\right) = \delta \int_{Z_{LFC}}^{Z_{LNB}} \frac{T_{ve} - T_{vp}}{T_{vp}} \tag{5}$$

where, δ is the acceleration due to gravity, T_{ve} and T_{vp} are the virtual temperatures of environment and parcel, respectively. Z_{LNB} And Z_{LFC} are the heights of the level of neutral buoyancy and the level of free convection, respectively [33].

In this study, the dominant synoptic event affecting the unique hail occurrence of March 30th in 2015 is the blocking phenomenon, the characteristics of which are described below: There exist some criteria to identify the blocking system [34]:

1) The main stream of west winds should change to two divisions.

2) Each division transforms specific air mass.

3) The two-division streams should contain at least longitude of 45˚.

4) A change from superior equatorial flux to inferior meridional flux should be observed in the two-divided divisions.

5) Finally, this pattern should last within a specific continuity for 10 days.

In addition to these characteristics, the quantitative methods could be adopted in identifying the blocking system; thus, before running typical qualitative studies to determine the systems, the existence of blocking system is tested in a quantitative manner. The equation below is applied to identify the blocking system, where if the amount of $C \le 0$ is equal to or less than zero, air stream has the potential to evoke blocking system, otherwise, west winds blow normally [35]. These equations suggest that if the west winds blow faster, the length of stationary waves increase.

$$C = U - \frac{\beta * Ls^2}{4\pi^2} \tag{6}$$

where, C is the eastwards propagation of Rossby waves

U is the speed of the initially uniform westerly flow of air (m/s)

Ls is the stationary wavelength (km)

Here, the β Coefficient is calculated through Equation (7):

$$\beta = \frac{2\omega * \cos\phi}{R} \tag{7}$$

where, ω is the earth's angular velocity equal 7.29×10^{-5} rad/s

R is the radius of earth (kilometer), and ϕ: latitude (degree)

Ls is the stationary wavelength (km) which is calculable for various latitudes and wind speeds according to Equation (8).

$$Ls = 2\pi - \sqrt{\frac{U}{\beta}} \tag{8}$$

where, U is calculable by the use through Equation (9):

$$U = \frac{\beta * L^2}{4\pi^2} \tag{8}$$

where, L is the length of real wave, calculated according to synoptic maps' scale.

3. Results and Discussion

The statistical analyses reveal that high concentration of hail occurrence in Tehran occurs during March-May, Table 2, between the hrs 6 - 18, Table 3. Between these hours of the day hail occurrence is due to sunshine and the heat generated thereof, the occurred instabilities at other relevant conditions like presence of cold layer in the lower layer of air mass during rainfall and rapid ascend of humid air mass. Assessing changes in hail occurrence time indicates that this occurrence increases in the transitional seasons of spring and fall, hence a fact corresponding the findings in [19]. Total days of hail occurrence at Mehrabad station, due to having long periodic stations and as the control stations, is 21. Monthly analyses make the spring months outstanding since the maximum instability due to the mountainous nature of the region (North and East of Tehran) which facilitates rapid ascending of air mass is subject to the topography of the region.

Table 2. Monthly change in hail occurrence at Mehrabad stations (1985-2015).

Month	Jan	Feb	March	April	May	Jun
Occurrence#	3	9	26	68	100	47
Month	July	Aug.	Sept.	Oct.	Nov.	Dec.
Occurrence#	31	22	19	46	14	9

Table 3. Hourly changes in hail occurrence at Mehrabad stations (1985-2015).

Station	hr	00	03	06	09	12	15	18	21
Mehrabad	Occurrence	37	14	12	22	51	79	106	62

According to Table 4, the lower the SHOW index (negative or approaching negative point) the more the floatation, thus an increase in atmospheric instability. The numerical values of this index in the designated day reveal a 5 digit reduction within less than 12 hrs at the occurrence region. The K index in the designated day at hour 00:00 GMT is recorded between 20% - 40% and the intensity thereof has increased the percentage to 60 - 80 at hour 12:00 GMT. This indicate an interval in CAPE for min 20 to max 80%.

The Boyden index indicates an increase in probability and prediction of thunderstorm occurrence at Mehrabad station in the same day. As for KO index, the more negative, the high the floatation thus an increase in atmospheric instability. the probability of thunderstorm occurrence, according to this index in the designated date at hour 00:00 GMT, was +10.4 while at hour 12:00 it decreased drastically down to −4.5, thus a high probability in thunderstorm occurrence. By assessing the SkewT thermodynamic diagram, Figure 2, at Mehrabad station at 12:00 o'clock UTC of the subject date indicate that the relative humidity (RH) among the atmospheric layer constitute 13% min at 532 hPa and 91% max at 600,615 and 647 hPa levels and dew point temperatures within −36.5 to +10.4˚C range. This condition illustrates the humidity distribution process up to 6 km height from earth's surface the value of which diminishes at upper layers. This fact indicates the RH state at air flows bellow 850 hPa has major contribution in humidity source distribution in the region. The CAPE volume at 12:00 o'clock in Mehrabad station is reported at 4 J/Kg (far right, CAPE diagram in blue). Calculation of all indexes and the dynamic are reflected in the diagram indicating that the intensity level and convective energy is moderate. These conditions indicate that in the date of concern, all conditions were fit to support hail occurrence.

The maps are illustrated according to hourly data, and hail phenomenon of 30th March of 2015 is analyzed according to meteorology codes for studying the hail precipitation thermodynamic and synoptic states. The map of sea level pressure in 30th March of 2015 is drawn in Figure 3(a), where two low-pressure centers of 1) 1008 hPa formed above the north of Arabia and east of Black Sea, and 2) a low-pressure system with 980 hPa in center with northwest-southeast orientation formed in north of Europe and west of Russia, with a developing orientation towards northwest of Iran. A strong high-pressure system with 1040 hPa in center exists in north of Caspian Sea and Lake Balkhash, with developing towards northern area of Tehran province. The study area is subject to these

Table 4. Assessing the occurrence and intensity of thunderstorm in March 30, 2015.

Index	00:00 o'clock	12:00 o'clock
SI	6	1.1
K	24.5	30.8
Boyden	96	94.8
KO	10.4	−4.5
CAPE	-	4

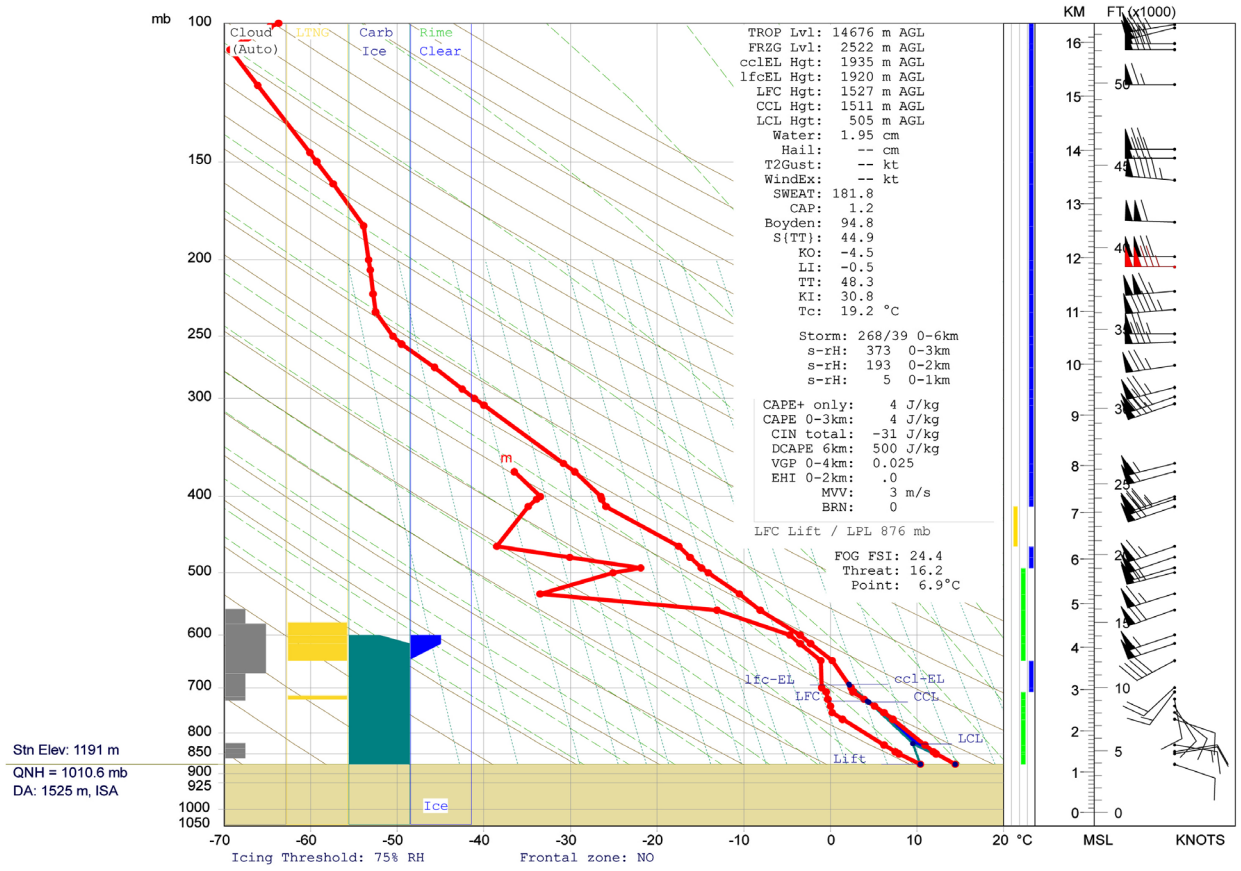

Figure 2. SkewT thermodynamic diagram, Mehrabad station, at 12 o'clock UTC in March 30, 2015, the components consist of: wind (m/Sec.), RH (%), temperature (˚C), CAPE (J/Kg).

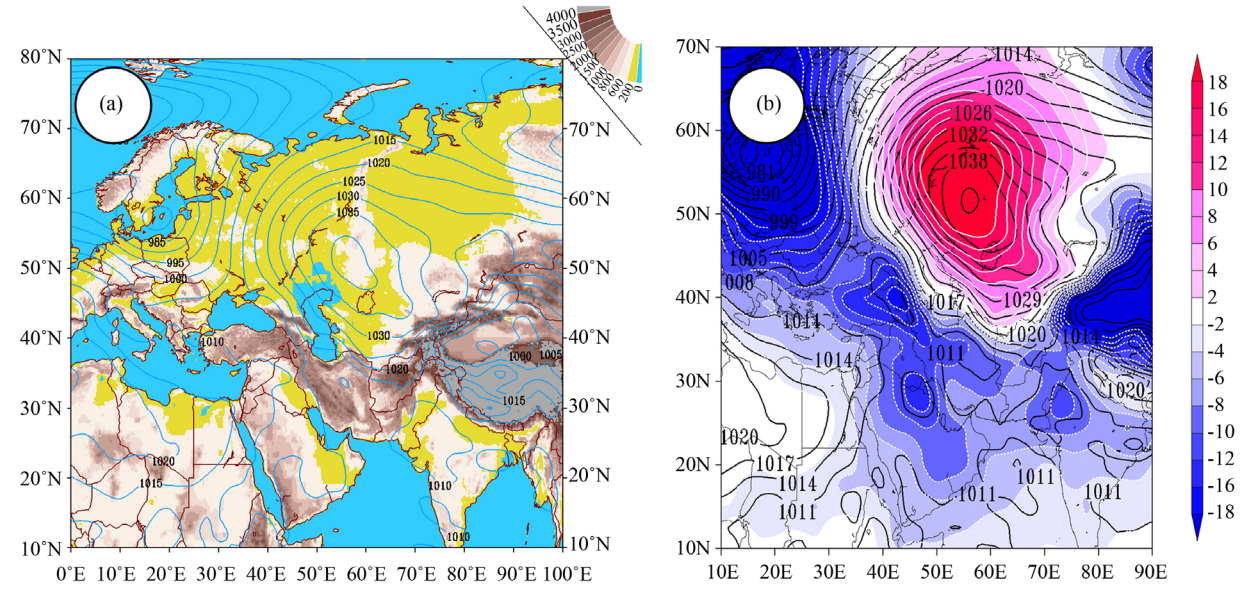

Figure 3. The sea level pressure: (a) the map of sea level pressure on March 30, 2015 and (b) the anomaly map of the same.

pressure centers, development of northern high-pressure cold weather and its collision with southern low-pressure warm weather which develop a high pres-

sure gradient which, as a local thermal front, causes the transfer of instable streams over Tehran province. The anomaly of sea level in day of concern is shown in Figure 3(b), below where a strong positive highly pressurized center is covering Siberia with a stronger long term mean. An anomaly negative core is observed at the west and SW Iran, indicating instability in the region and another anomaly is observed at the West and NW over Mediterranean. In the North of Afghanistan, there is another strong negative core covering a NE Iran as well, and since it is at high geopotential hight it is weaker than the average of its kind. Another negative anomaly is observed beginning from SE Iran crossing Arabia peninsula in parallel to Red sea with NS orientation.

As observed in Figure 4(a), a low hight center with 1165 geopotential of 850

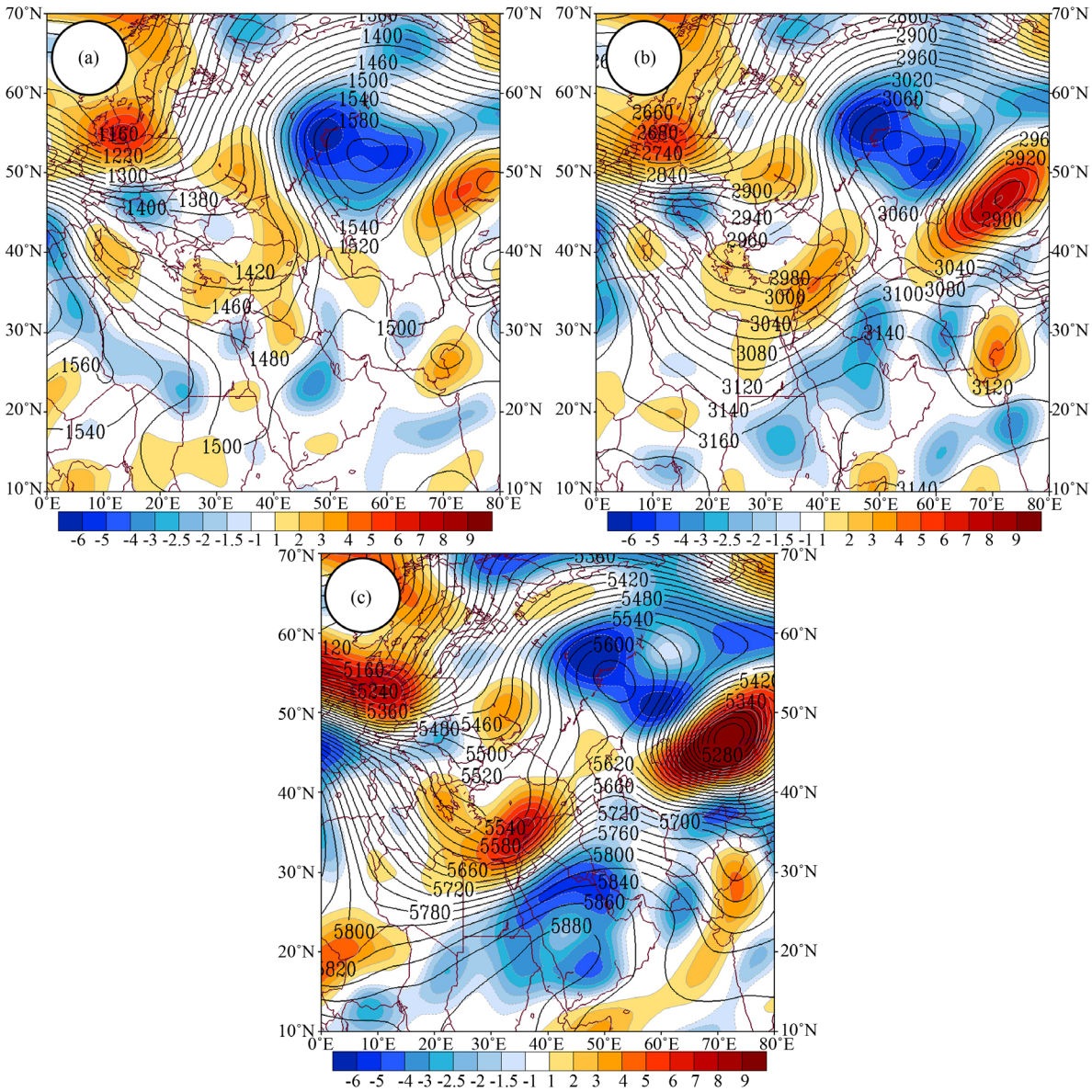

Figure 4. The combined geopotential high and a rotating map of March 30, 2015 (a) 850 hPa level, (b) 700 hPa level and (c) 500 hPa level.

hPa in a NW-SE orientation is extended from North of Europe to the central region of Iran. It extended on Soudia Arabia while the trough oriented from north to sought direction. According to sea level map a high geopotential center a high elevated pressure of 1590 geopotential with N-S orientation is alongated towards eastern regions of Tehran province with S and W.

This phenomenon verifies the heat overshoot at this level. At 700 hPa, **Figure 4(b)** is in accordance with the lower levels and the deployment of highly elevated geopotential at 3100 meter in Caspian Sea north reveals a blocking in the shape of Omega. The positions of the study are between Northern highly elevated and low elevated N Europe together with the expansion of hot flows due to clockwise rotation of the high elevations geopotential at 3175 meter closed center on Arabia provide the grounds for thunderstorm and hail occurrence. At this level a very deep trough covers the whole central Mediterranean to central Iran. It is observed that in this study zone in the best of conditions confronts trough by showing the flows/current in SW orientation. In **Figure 3(c)** at 500 hPa level the same lower patterns of levels are illustrated. The changes here are due to stronger low elevated centers in N Europe leaning towards higher latitudes with a backward bent over Arabia, where the Caspian Sea ridge becomes dipper and expanded, indicating a strong high pressure system overwhelming the region which leads to ascending promotion and development of an atmospheric bent pressure on Tehran province.

At all levels there exists negative rotation which overwhelms the Arabia and Siberia high pressures and an increase in the levels propagates this pressure. These negative rotations show the advance of the high pressure tongue towards Iran and Tehran in specific. As observed in **Figures 4(a)-(c)** the superficial rotations are positive while the core of the same is negative and this comparing with [36] findings. By comparing these maps it becomes evident that the negative divergence fields at lower atmospheric level are replaced with these positive counterparts at intermediate and upper atmospheric level. Coordination of these conditions in 30 March, 2015 indicate an appropriate condition for the air dynamic on Tehran atmosphere to ascend and the same rapid dynamic ascending to the intermediate and upper atmospheric level, eventually leading to the hail occurrence in the day. Higher proportional rotation developed a very deep level which by its Eastward movement developed the proportional dynamic conditions for ascending in the study zone.

Blocking system distorts the usual process of western streams and, it divides the stream into two divisions, consequently the dominant flux changes from equatorial to meridional position. Blocking system is distinguished from components of west winds as a warm and constant high-pressure (with a very slow movement). Blocking systems are usually formed from warm and high tongues which advects warm weather from tropical regions to latitudes above. Blocking systems cause deviations in the west winds' path and polar front transformation towards the east with different outcomes in different regions, leading to no rain precipitation, thus, drought in some regions and in others to increase in rain

precipitation. Analysis of synoptic maps of earth surface indicate that through domination of blocking anti-cyclones, the advection warm weather penetrates to higher latitudes unexpectedly and push cold weather to the subtropic region. Considering these meridian streams, particular regions affected by blocking system will enjoy annoying warmth or coldness, depending on the situation. In some cases, the repeated occurrence of blocking patterns is able to change the general characteristics of the given season [34].

The meridian west winds' speed map at 300HPA height is studied to analyze the direction of advection in air streams, and the map of air stream lines at 500HPA height is studied to determine the blocking system quality effect on the western streams **Figure 5** & **Figure 6**. As observed in **Figure 5**, due to formation of blocking system, the stream of western winds have become highly meridional, and by disturbing the usual flow of west winds, it sets the two contours of 563 and 560 geopotential decameter apart, in a manner that the closed contour of 560 geopotential decameter over Mediterranean Sea divides into the west winds in two divisions: one parallel to contour 563geopotential decameter which entered Iran in direction of northwest-southeast and affected mostly the northern hemisphere of the country, and the other deviated parallel to contour 560 geopotential decameter and affected mostly the north of Caspian Sea **Figure 4(c)** and **Figure 6(b)**; stream lines). This state causes the cold weather convection in northern hemisphere of Iran. Thus, most of Tehran stations have experienced the least temperature on 30th March due to flowing of cold weather from above latitudes **Figure 5** & **Figure 6**. Examining the average MSL map on 30th March of 2015, a high-pressure center with central pressure of 1040 hPa is observable over Moscow and Siberia the tongue of which encloses Caspian Sea and Tehran; the placement of curve 1010 hPa to northern half of Iran is in agreement with

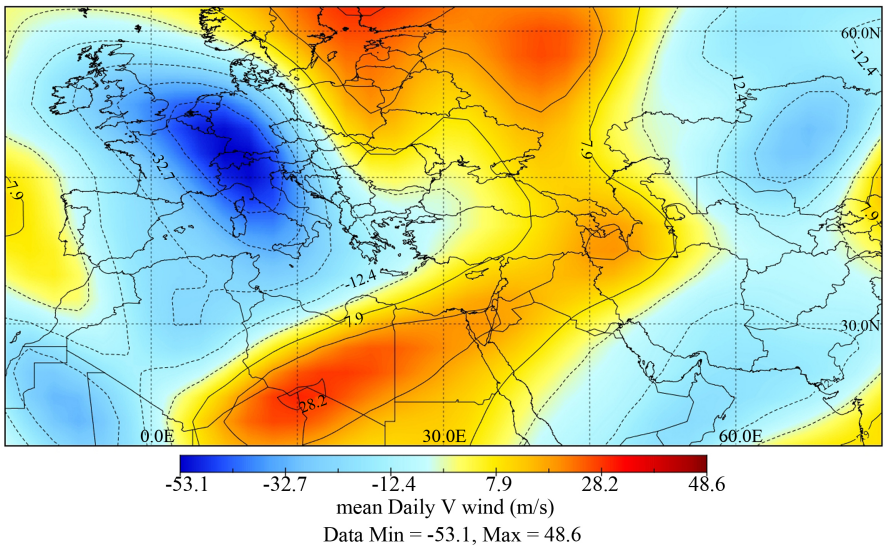

Figure 5. Map of speed of meridian factor (V) of wind in level 300 HPA on March 30th in 2015 (meter per second), the dotted line is in the direction of decreasing speed of cold advection, and soild line is the direction of increasing speed of warm advection.

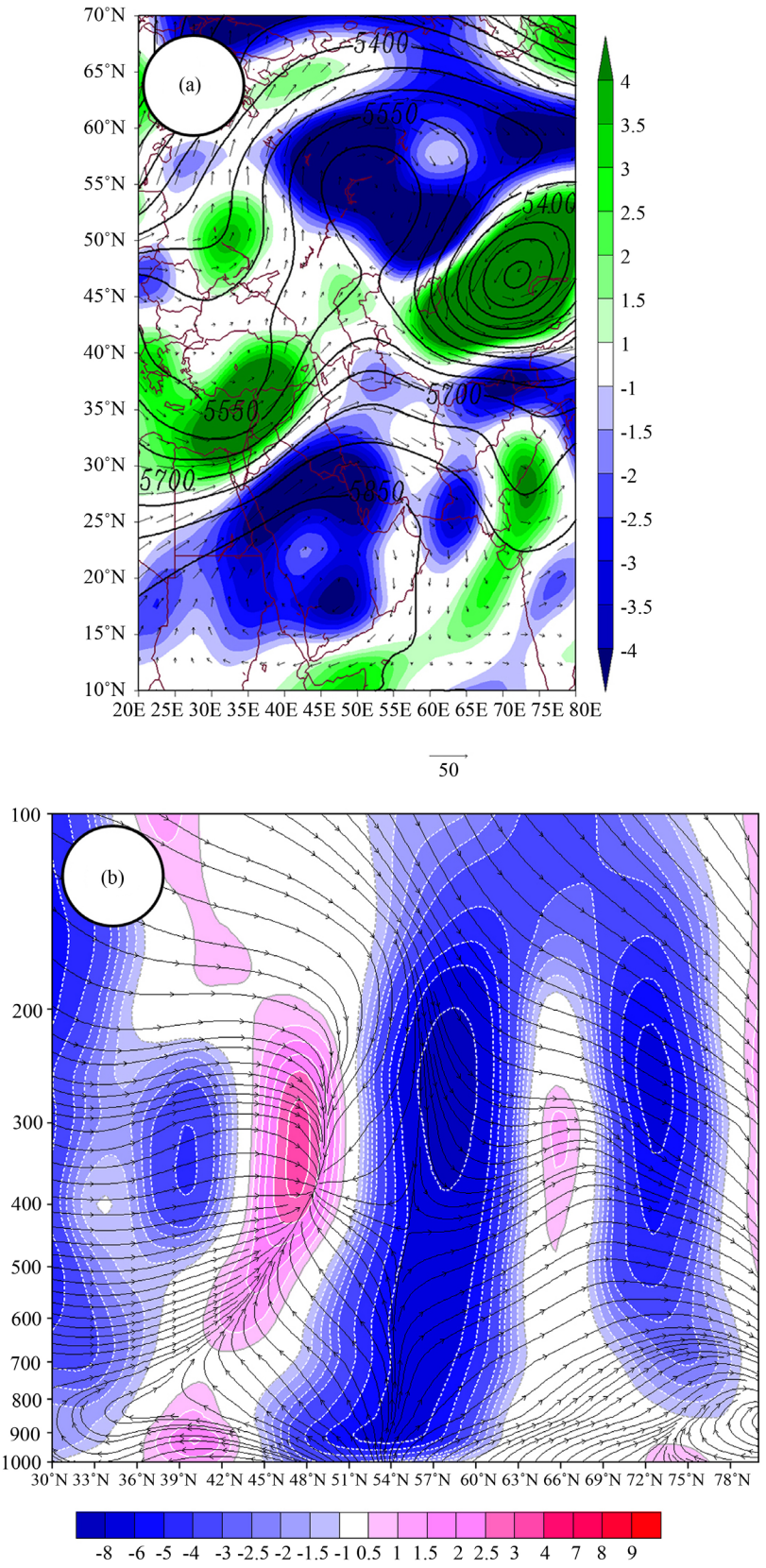

Figure 6. Compound map of average height of geopotential level of 500 HPA (a) speed of wind (meter per second); (b) lines of stream on March 30th in 2015.

severe coldness in most stations of Iran.

To test the presence of blocking system as a dominant control pattern of atmospheric conditions in study period, the amount of replacement of wave pattern of west winds toward east (C) is calculated. If replacement of wave pattern is towards east, C will be positive; and if towards west, C will be negative. The reason here is that the wave pattern speed replacement, together with Earth's rotation, have decreased so much that it is slower than that of the Earth. If there is no replacement in wave pattern, C will become zero. The obtained results reveal that C on March 30th 2015 was negative and equal to −0.005 meter per second. This phenomenon proves the reduction of movement of west winds. This fact proves the settlement of blocking system on March 30th in 2015. The domination of blocking system on the subject day corresponds to what is observed in **Figure 4**.

The maps of the vertical air speed at all levels from 1000 to 100 hPa for two days prior and one day after hail occurrence are drawn for accurate assessment of this occurrence. As observed, a negative omega (In blue) appear in 29th March 2015 between orbits 28 and 42 Eastern degrees. Assessing the dynamic quantity reveals that vorticity volume reaches 7^{-5} S^{-1} (m/Sec.), **Figure 6(a)** at all times with the vertical air speed at 0.3 and 0.08, **Figure 7(a)** also shows The negative omega center field within the above mentioned orbit where is not replaced, while in the middle of positive omega center it follows a downward vertical velocity at 0.5 with a relatively strong divergence in 49 - 59 E degree at 1000 - 100 hPa Eastward with maximum vorticity equal to 9×10^{-5} m/Sec. On March 29th this speed is reduced to 5×10^{-5} m/Sec. and is placed between 800 - 200 hPa.

The next day , when hail storm occurred, a high geopotential center with the least negative vorticity volume between -1×10^{-5} to -6×10^{-5} m/Sec. is formed in between 80 to 500 hPa levels. The lower vorticity volume develops very deep ridge. In this specific day all across the orbit a prevailed negative omega locates at 40 - 80 Eastern degrees. The maximum negative omega is between 40-50 Eastern degrees with its center with minimum volume of velocity > −0.5 at 800 - 300 hPa. On March 31th the negative omega center has been subject to many displacements **Figure 7(d)** between 60 - 80 degrees of orbit, thus, a change or complete ejection from the region under study. At 17 fold levels the negative omega center is located on NW Iran. The outstanding point here is that the strength level of convective and vertical upward speed of air near earth's surface is evident. At 500 hPa, **Figure 7(c)** the vertical air speed on the region is −0.34 Pascal/Second. Beyond 800 hPa level, the negative omega field expands to a point that covers the northern half of Iran. The negative volume of vertical velocity from 1000 to 500 hPa, with the same spatial expansion in the E and SE of the upper atmospheric trough of levels are located over earth surface low pressure level.

The combined maps of humidity flow and the geopotential height at 4 fold levels in March 30th are illustrated (8). In **Figure 8(a)**, the humidity flow is at 925

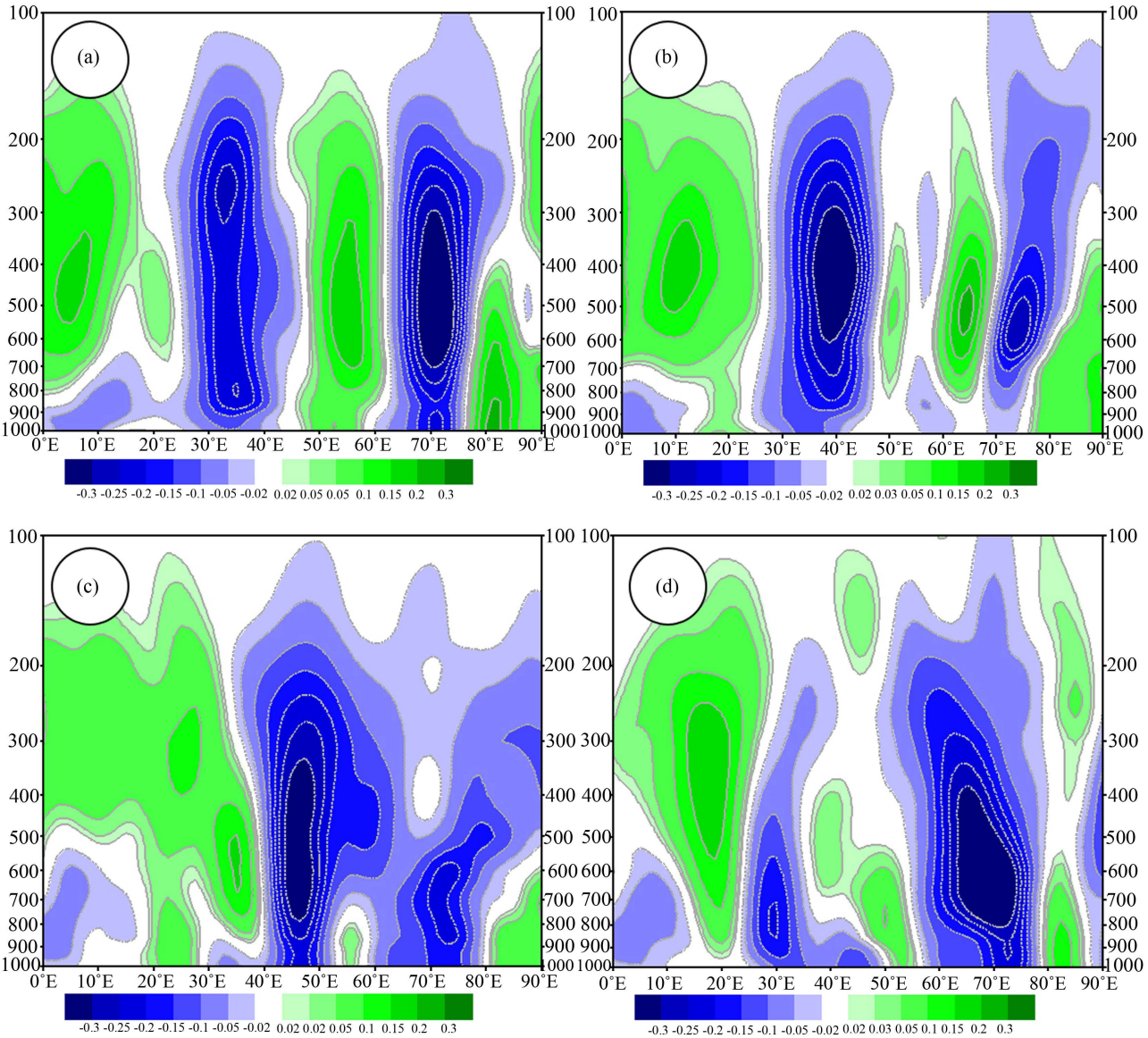

Figure 7. Vertical atmospheric speed p/hp (omega): (a) March 28th, (b) March 29th, (c) March 30th and (d) March 31st, 2015.

hPa level, at low elevation in the north of Arabia and half of south Iran with the orbital contour generated from high elevation on Mediterranean Sea as to humidity flow with an overshooting towards the S and SW with prevailing components towards Tehran. The Arabian, Red, Mediterranean seas and the Persian Gulf provided humidity at 925 hPa level. In **Figure 8(b)** humidity flow at 850 hPa level the Arabia sea transmits less humidity and influenced by expansion of low elevated trough toward the southern latitude up to central Arabia allows the Mediterranean humidity to be combined with that of the Red sea and Persian Gulf which after passing over the hot territory of Arabia is transferred over the subject region in an anticlockwise manner. At 700 and 500 hPa levels **Figure 8(c)** & **Figure 8(d)** the contribution of Arabia and Mediterranean Sea in providence and transfer of humidity is eliminated while the opposite holds true for

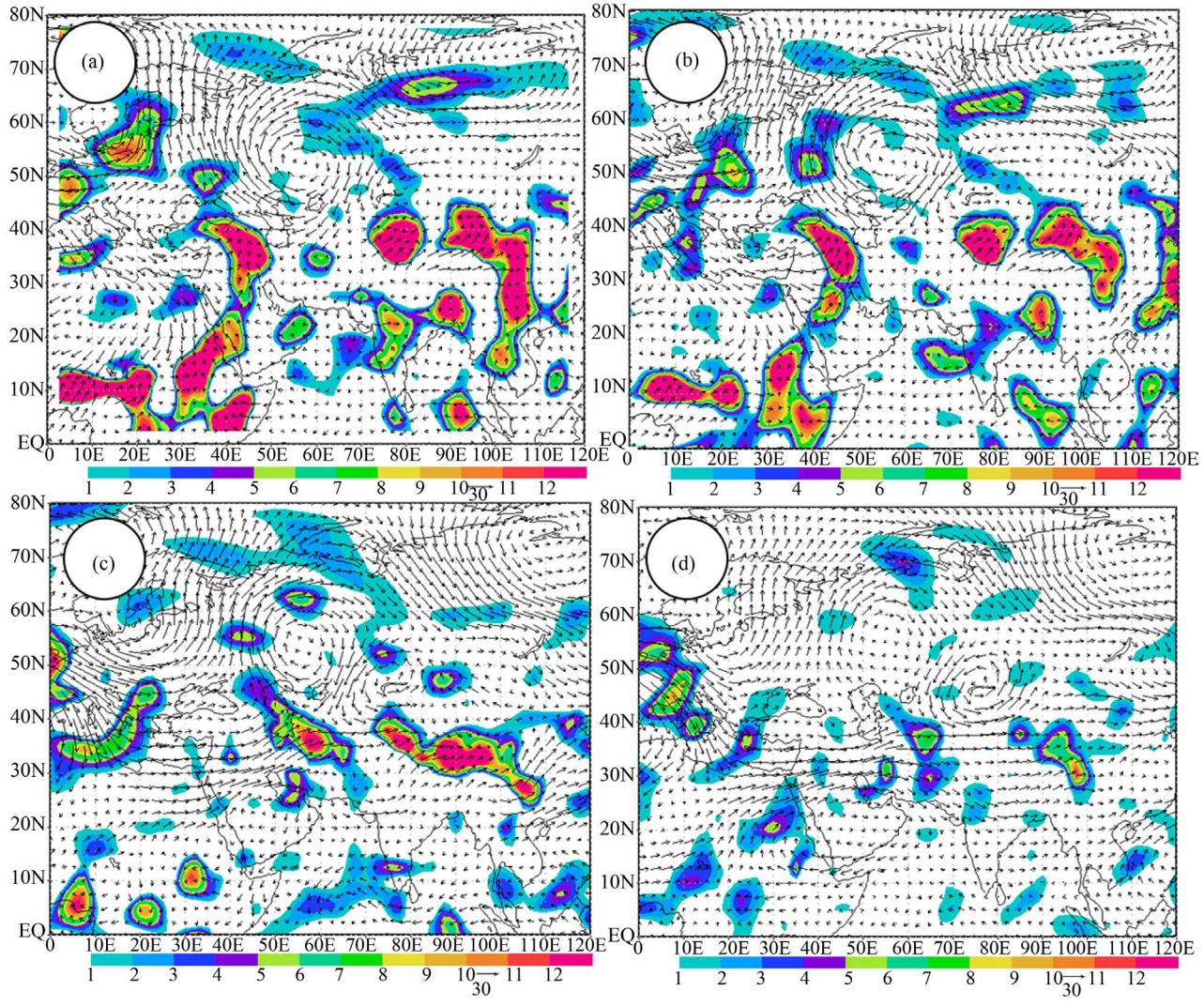

Figure 8. Humidity flow on March 30, 2015: (a) 925 hPa, (b) 850 hPa, (c) 700 hPa and (d) 500 hPa.

Red sea and Persian Gulf, with a high contribution to hailstorm occurrence in the study zone through all countries and reactions thereof. Through research of the humidity flow maps it is revealed that the Arabian Sea, with the highest volume in providing and overshooting humidity is dominant here.

The maps of jet stream of the occurrence day at 250 and 300 hPa are shown in Figure 9. These maps show the presence of a very strong jet stream with sub-tropical SW-NE orientation passing over Red Sea, Mediterranean sea and Persian Gulf over Iran, Tehran province in specific. Existence of such jet stream introduce the cyclone-generating conditions in the region in a rapid manner with control core of speed of 60 - 70 m/Sec. at 250 and 300 hPa, respectively which contribute to restoring instability, Figure 9. this condition is in accordance with a high divergence of the region in the E of trough axis, the maps regarding omega (vertical speed) verify this fact. This phenomenon leads to formation of unstable atmosphere with bent pressure in the zone under study.

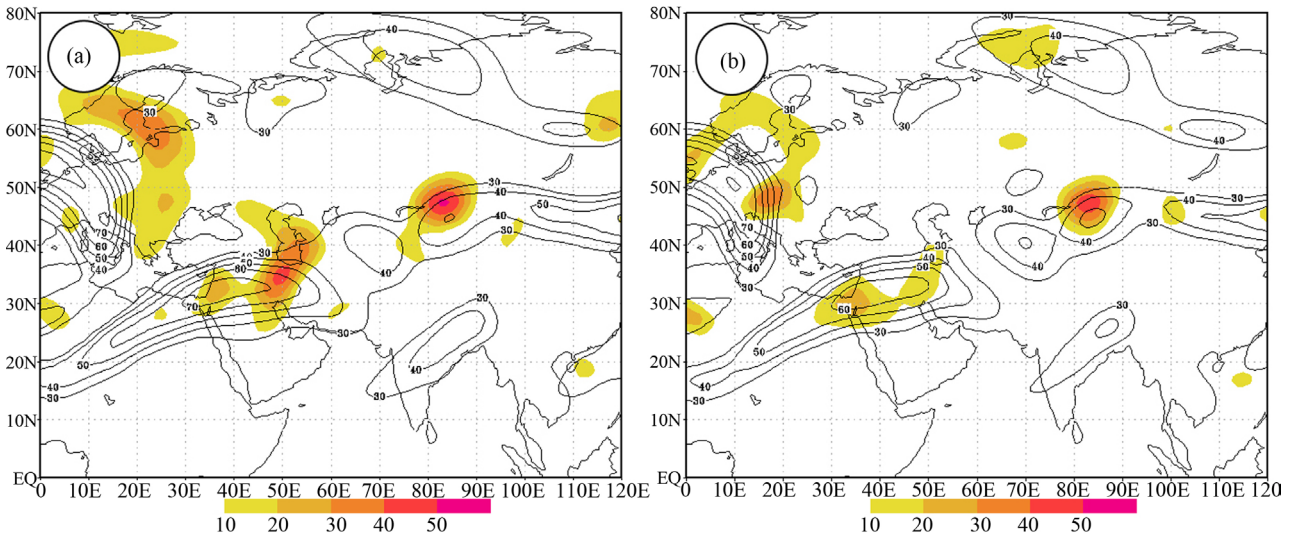

Figure 9. The jet stream map at (a) 250 hPa and (b) 300 hPa in the day of hail occurrence.

The liquid, icy clouds path, the cloud light thickness and the temperature above the cloud is obtained and calculated through Moddis Aqua, Terra and AIRS measuring apparatus are shown in **Figure 10**. As observed in **Figure 10(a)** the liquid clouds path with maximum 1739 g/m^2 is located in the E of black sea with the tongues stretched from NW and N towards the central parts of Iran. In Tehran this volume reached 241 g/m^2. The states of the icy clouds path, **Figure 10(b)** is similar to that of the liquid clouds while, here, in the west of Turkey and North Mediterranean has a great contribution with the maximum index of 2174 g/m^2 and a minimum of 1 g/m^2 in deserts around Hijaz and Red sea. The index of icy clouds in Tehran province is 643 g/m^2, indicating conditions for hail of considerably big size (recorded as big as ping-pong ball). The light-thickness of this cloud is shown in **Figure 10(c)**, with the thickest portion at NW of Iran and thin parts of SE Black Sea. This thickness was recorded at 19.52 micron in the day of hail occurrence.

The temperature above the cloud above the city of Tehran reached −45.75˚C which verify the hail occurrence a considerable part of Iran. The above cloud temperature in Iran in that given day is recorded as negative between the orbits at 50 - 60 degree towards E which is recorded a maximum for Tehran, Mazandaran, Golestan, Qum and Isfahan provinces in relation to other parts of Iran.

4. Conclusions

Climatic extreme event is considered as a warning to environment. Hail is an important extreme event that due to climate change its occurrence has intensified in recent years causing damages. It is revealed in this study that hailstorm occurrence on 30th of March is as pervasive and unexpected event justified studying the 9 codes of current weather (WW) during 1985 to 2015 in Tehran.

To assess the situation causing hail storm, the instability indices and synoptic climate patterns are studied. The results indicate that hail and heavy rainfall on

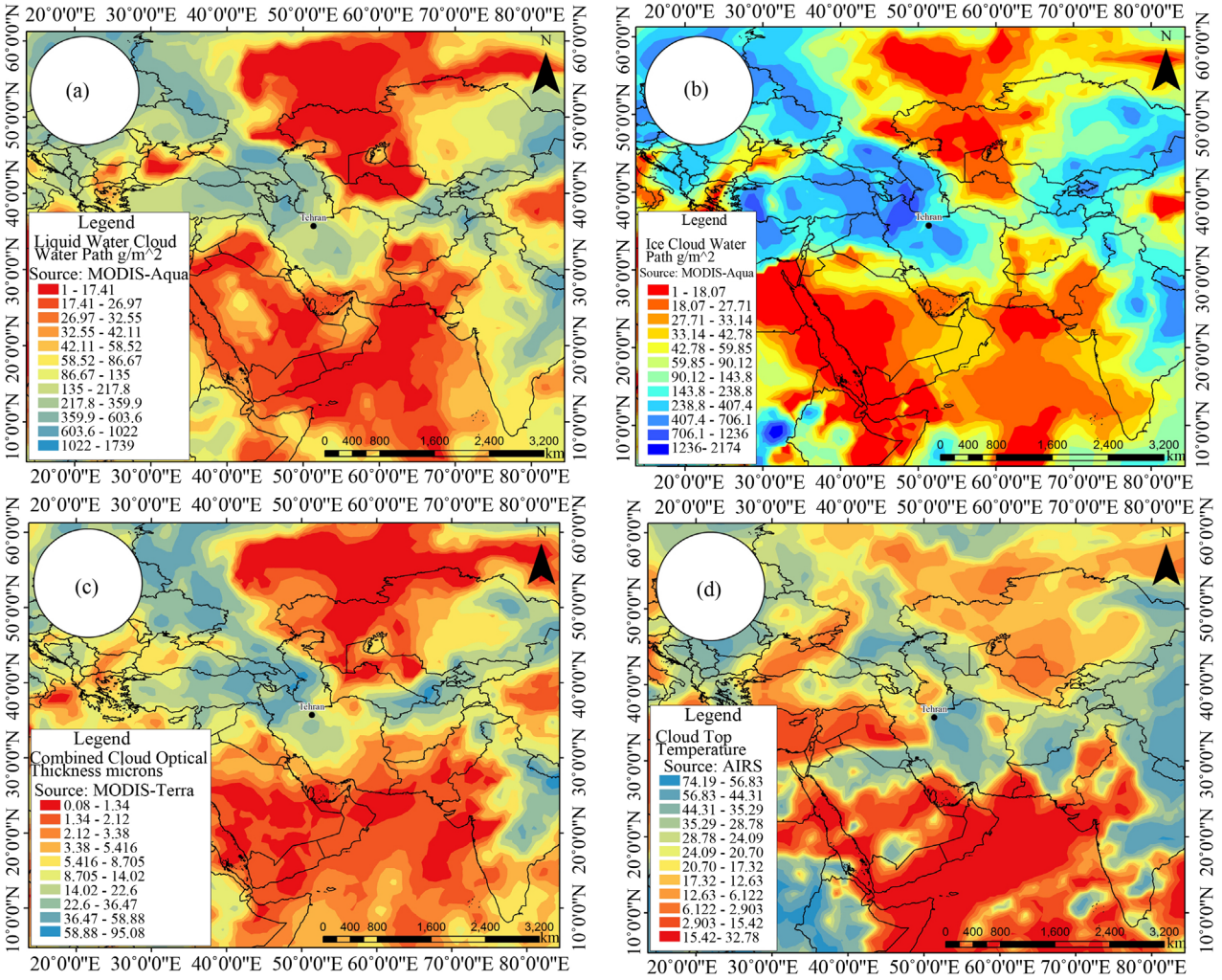

Figure 10. (a) Ice cloud water Path g/m^2; (b) Liquid water cloud water path g/m^2; (c) Combined cloud optical thickness microns; (d) Cloud top temperature ˚C.

30th of March recorded in most stations in Tehran province are of the southern and western stations like Mehrabad, Rey, Varamin, Geophysic and Shahriyar was a prince. On this day, most of northern, central and western Iran faced heavy rainfall.

The five instability indices indicate that instability was high in the afternoon; which added to the instability in upper level of atmosphere and provided the potential to support and strengthen the hail occurrence in Tehran.

The obtained results here indicate the synoptic assessment and the instability indexes by applying data supplied by satellite contribute to diagnosis of the formation and occurrence mechanisms of hailstorms that led to flooding. Being equipped with appropriate knowledge regarding natural disasters caused by climatic elements can reduce the destruction rate to a certain degree. Accuracy and importance of instability indices in this study is in agreement with that of the [33] who applied the mentioned five indices for the monsoon region. These indices can be applied at high levels of confidence to predict the occurrence of hail

in Iran.

Index K indicates the likelihood of thunderstorms in the afternoon is up to 80%. The thermodynamic results of Skwt diagrams of Mehrabad station in Tehran shows that the relative humidity of the atmospheric layers change between minimum of 13% at 532 hPa level and a maximum of 91% at 600 to 647 hPa level. The dew point temperature oscillates between −36.5 to 10.4˚C.

According to sea level pressure maps, the establishment of high-pressure cell in the north of Caspian and Balkhash Sea with 1040 hPa central pressure affected north Iran. At this time, a low pressure core with the 1008 hPa central pressure on the north south west Iran and northern Saudi Arabia extends its warm air toward Tehran and dealing with the cold high-pressure north while cause intensive pressure gradient and event is unstable.

The geopotential elevation maps at 700 - 500 hPa levels indicate omega shape blocking system's positioning in accordance with earths' high pressure levels beginning from south Russia ending in eastern half of Iran. In the west of this blocking the low elevated elongation at north of Europe towards NW-SE and the positioning of the study area in front and east axies of the tough and expansion of tough on the southern water sources like the Red Sea and Persian Gulf divert southern and western hot flows towards Tehran province. The jet stream maps at 200 and 300 hPa levels almost follow the same path subject to the negative omega field with a core of 70 m/Sec. speed in the north of Red Sea and Arabia leading to intense instability. The total atmospheric humidity (precipitance water) maps reveal existence of maximum humidity core of 45 gr/kg on Tehran. Humid wind flow indicate that at 1000 and 850 hp level the Red sea, Arabian sea, Persian Gulf and Mediterranean sea, had their share in promoting and straitening the humidity necessary for hailstorm. At 500 and 700 hPa level the Arabian Sea and Mediterranean Sea had no contribution in humidity transfer inside the system while Red sea and Persian Gulf had slight contribution in this respect. Through this study, it is revealed that influence of high and low pressure system of the Northern latitude near the North Pole and its extension on Iran and hot and humid resources of the south led to intensified pressure gradient, thus devastating hailstorm and flooding thereof.

The available studies like [37] and [38] just like this study verify that the intensive synoptic mechanism of upward tough motion and the air fronts have significant contribution in hail occurrence. The contribution of synoptic and microphysics of the clouds, the cloud upper temperature in specific, are verified in hail occurrence [20].

References

[1] Etkin, D. and Brun, S.E. (2001) Canada's Hail Climatology. Institute for Catastrophic Loss Reduction (ICLR), Toronto.

[2] Zhang, C., Zhang, Q. and Wang, Y. (2008) Climatology of Hail in China: 1961-2005. *Journal of Applied Meteorology and Climatology*, **47**, 795-804. https://doi.org/10.1175/2007JAMC1603.1

[3] Longley, R.W. and Thompson, C.E. (1965) A Study of Causes of Hail. *Journal of Applied Meteorology*, **4**, 69-82. https://doi.org/10.1175/1520-0450(1965)004<0069:ASOCOH>2.0.CO;2

[4] Das, P. (1962) Influence of Wind Shear on the Growth of Hail. *Journal of the Atmospheric Sciences*, **19**, 407-414. https://doi.org/10.1175/1520-0469(1962)019<0407:IOWSOT>2.0.CO;2

[5] Dessens, H. (1960) Severe Hailstorms Are Associated with Very Strong Winds between 6,000 and 12,000 Meters. *Proceedings of the Cloud Physics Conference on Physics of Precipitation*, Woods Hole, 3-5 June 1959, 333-338.

[6] Rinehart, R.E. (1991) Radar for Meteorologists. University of North Dakota, Office of the President.

[7] Chatterjee, P., Pradhan, D. and De, U.K. (2008) Simulation of Hailstorm Event using Mesoscale Model MM5 with Modified Cloud Microphysics Scheme. *In Annales Geophysicae*, **26**, 3545-3555. https://doi.org/10.5194/angeo-26-3545-2008

[8] IPCC (2013) Fifth Assessment Report of the Intergovernmental Panel on Climate Change. Assessment Report, Intergovernmental Panel on Climate Change, New York.

[9] Allen, M.R., Barros, V.R., Broome, J., Cramer, W., Christ, R., Church, J.A. and Edenhofer, O. (2014) IPCC Fifth Assessment Synthesis Report-Climate Change 2014 Synthesis Report.

[10] Bindoff, N.L., Stott, P.A., AchutaRao, K.M., Allen, M.R., Gillett, N.J., Gutzler, D. and Mokhov, I.I. (2013) Detection and Attribution of Climate Change: From Global to Regional.

[11] Trenberth, K.E., Jones, P.D., Ambenje, P., Bojariu, R., Easterling, D., Tank, A.K. and Soden, B. (2007) Observations: Surface and Atmospheric Climate Change, Chap. 3 of Climate Change 2007: The Physical Science Basis. Contribution of Working Group I to the Fourth Assessment Report of the Intergovernmental Panel on Climate Change, 235-336.

[12] Vellinga, P., Mills, E., Berz, G., Bouwer, L., Huq, S., Kozak, L.A. and Bruce, J. (2001) Insurance and Other Financial Services. In: *Climate Change*, 417-450.

[13] Misra, P.K. and Prasad, S.K. (1980) Forecasting Hailstorm over India. *Mausam*, **31**, 385-396.

[14] Vinet, F. (2001) Climatology of Hail in France. *Atmospheric Research*, **56**, 309-323.

[15] Giaiotti, D., Nordio, S. and Stel, F. (2003) The Climatology of Hail in the Plain of Friuli Venezia Giulia. *Atmospheric Research*, **67**, 247-259.

[16] Schuster, S.S., Blong, R.J. and Speer, M.S. (2005) A Hail Climatology of the Greater Sydney Area and New South Wales Australia. *International Journal of Climatology*, **25**, 1633-1650. https://doi.org/10.1002/joc.1199

[17] Chromá, K. (2006) Temporal and Spatial Variability of Hailstorms in Moravia and Silesia (Czech Republic) in the 19th-20th Centuries. *In Geophysical Research Abstracts*, **8**, 04367.

[18] Kunz, M., Sander, J. and Kottmeier, C. (2009) Recent Trends of Thunderstorm and Hailstorm Frequency and Their Relation to Atmospheric Characteristics in Southwest Germany. *International Journal of Climatology*, **29**, 2283-2297. https://doi.org/10.1002/joc.1865

[19] Ghavidel, Y., Baghbanan, P. and Farajzadeh, M. (2017) The Spatial Analysis of Thunderstorm Hazard in Iran. *Arabian Journal of Geosciences*, **10**, 123. https://doi.org/10.1007/s12517-017-2902-7

[20] Buckley, B.W., Leslie, L.M. and Wang, Y. (2001) The Sydney Hailstorm of April 14,

1999: Synoptic Description and Numerical Simulation. *Meteorology and Atmospheric Physics*, **76**, 167-182. https://doi.org/10.1007/s007030170028

[21] Sioutas, M.V. and Flocas, H.A. (2003) Hailstorms in Northern Greece: Synoptic Patterns and Thermodynamic Environment. *Theoretical and Applied Climatology*, **75**, 189-202. https://doi.org/10.1007/s00704-003-0734-8

[22] Nieto, R., Gimeno, L., de La Torre, L., Ribera, P., Gallego, D., García-Herrera, R. and Lorente, J. (2005) Climatological Features of Cutoff Low Systems in the Northern Hemisphere. *Journal of Climate*, **18**, 3085-3103. https://doi.org/10.1175/JCLI3386.1

[23] Schlatter, P.T., Schlatter, T.W. and Knight, C.A. (2008) An Unusual Hailstorm on 24 June 2006 in Boulder. Colorado Part I: Mesoscale Setting and Radar Features. *Monthly Weather Review*, **136**, 2813-2832. https://doi.org/10.1002/joc.1199

[24] Picca, J. and Ryzhkov, A. (2012) A Dual-Wavelength Polarimetric Analysis of the 16 May 2010 Oklahoma City Extreme Hailstorm. *Monthly Weather Review*, **140**, 1385-1403. https://doi.org/10.1175/MWR-D-11-00112.1

[25] Iribnews (2015) 125 Billion Hail Damage. (In Persian) http://www.iribnews.ir/fa/news/79601

[26] WMO (2015) Manual on Codes. International Codes, Volume I.1. Annex II to the WMO Technical Regulations, Part A—Alphanumeric Codes, Publications Board, Switzerland.

[27] Gottlieb, R. (2009) Analysis of Stability Indices for Severe Thunderstorms in the Northeastern United States.

[28] Showalter, A.K. (1953) A Stability Index for Thunderstorm Forecasting. *Bulletin of the American Meteorological Society*, **34**, 250-252.

[29] Haklander, A.J. and Van Delden, A. (2003) Thunderstorm Predictors and Their Forecast Skill for the Netherlands. *Atmospheric Research*, **67**, 273-299.

[30] Boyden, C.J. (1963) A Simple Instability Index for Use as a Synoptic Parameter. *Meteor le Mag*, **92**, 198-210.

[31] Andersson, T.A., Andersson, M., Jacobsson, C. and Nilsson, S. (1989) Thermodynamic Indices for Forecasting Thunderstorms in Southern Sweden. *Meteorological Magazine*, **118**, 141-146.

[32] Glickman, T.S. (2000) Glossary of Meteorology. American Meteorological Society.

[33] Tyagi, B., Krishna, V.N. and Satyanarayana, A.N.V. (2011) Study of Thermodynamic Indices in Forecasting Pre-Monsoon Thunderstorms over Kolkata during STORM Pilot Phase 2006-2008. *Natural Hazards*, **56**, 681-698.

[34] McIlveen, R. (1992). Fundamentals of Weather and Climate. Oxford University Press, 398. https://doi.org/10.1007/978-1-4899-6892-0

[35] Barry, R.G. and Carleton, A.M. (2001) Synoptic and Dynamic Climatology. Routledge, London. https://doi.org/10.4324/9780203218181

[36] Dutton, J.A. (2002) The Ceaseless Wind: An Introduction to the Theory of Atmospheric Motion. Courier Corporation.

[37] Romero, R., Doswell, III. and Riosalido, R. (2001) Observations and Fine-Grid Simulations of a Convective Outbreak in Northeastern Spain: Importance of Diurnal Forcing and Convective Cold Pools. *Monthly Weather Review*, **129**, 2157-2182. https://doi.org/10.1175/1520-0493(2001)129<2157:OAFGSO>2.0.CO;2

[38] Tudurı, E., Romero, R., López, L., Garcıa, E., Sánchez, J.L. and Ramis, C. (2003) The 14 July 2001 Hailstorm in Northeastern Spain: Diagnosis of the Meteorological Situation. *Atmospheric Research*, **67**, 541-558.